SUPPORTING INFORMATION

Rapid Inhibition Profiling in *Bacillus subtilis* to identify the mechanism of action of new antimicrobials

Authors: Anne Lamsa[1,3], Javier Lopez-Garrido[1,3], Diana Quach[2], Eammon P. Riley[1], Joe Pogliano[1]*, Kit Pogliano[1]*

Affiliations: [1]Division of Biological Sciences, University of California, San Diego La Jolla, CA, USA.

[2]Department of Bioengineering, University of California, San Diego La Jolla, CA, USA.

[3]These authors contributed equally to this work.

[*]Co-corresponding authors. Email: kpogliano@ucsd.edu (K.P.), jpogliano@ucsd.edu (J.P.)

Keywords: antibiotic resistance; antibiotic discovery; mechanism of action, *Bacillus subtilis*; multidrug resistant bacteria

SUPPLEMENTARY METHODS

Plasmid construction.

ssrA* tag. The modified ssrA tag added has the amino acid sequence: (Ala Ser) Ala Ala Asn Asp Glu Asn Tyr Ser Glu Asn Tyr Ala Leu Gly Gly STOP, where the residues in parenthesis indicate a linker and not part of recognized tag.

pJLG44. This plasmid was constructed by assembling the following 4 fragments by Gibson Assembly (New England Biolabs): (i) the last 895 bp of the *murF* coding sequence (not including the stop codon) amplified with primers JLG-80 and JLG-81 from genomic DNA of *B. subtilis* PY79; (ii) *sfGFP-ssrA*Ωkan* fragment amplified with primers JLG-7 and JLG-77 from pJLG36[3]; (iii) a fragment of 937 bp corresponding to the region immediately downstream of the *murF* stop codon, amplified with primers JLG-82 and JLG-83 from genomic DNA of *B. subtilis* PY79; and (iv) a DNA fragment encompassing the origin of replication of pBR329, amplified with primers JLG-69 and JLG-70.

pJLG47. This plasmid was constructed by assembling the following 4 fragments by Gibson Assembly (New England Biolabs): (i) a fragment of 1025 bp encompassing the region upstream of *xylA* coding sequence and the first 128 bp of *xylA* coding sequence, amplified with primers JLG-106 and JLG-114 from genomic DNA of *B. subtilis* PY79; (ii) the kanamycin resistant gene of pEB19 [1] amplified with primers JLG-7 and JLG-97; (iii) a fragment of 997 bp corresponding to the last 161 bp of *xylA* coding sequence and the region immediately downstream, amplified with primers JLG-108 and JLG-109 from genomic DNA of *B. subtilis* PY79; and (iv) a DNA fragment encompassing the origin of replication of pBR329, amplified with primers JLG-69 and JLG-70.

pJLG60. To construct this plasmid, pJLG44 was amplified by inverse PCR with primers JLG-206 and JLG-209, which flank the *sfGFP* coding sequence. Both primers were phosphorylated at the 5' end, allowing religation of the PCR product. AS a result, the *sfGFP* coding sequence was removed and the *ssrA** fused directly to *murF*.

pJLG61. To construct this plasmid, pJLG49[3] was amplified by inverse PCR with primers JLG-206 and JLG-207, which flank the *sfGFP* coding sequence. Both primers were phosphorylated at the 5' end, allowing religation of the PCR product. AS a result, the *sfGFP* coding sequence was removed and the *ssrA** fused directly to *sigA*.

pJLG67. This plasmid was constructed by assembling the following 3 fragments by Gibson Assembly (New England Biolabs): (i) pJLG47 amplified with primers JLG-189 and JLG-190; (ii) *sspB** amplified with primers JLG-185 and JLG-186 from genomic DNA of *E. coli* K12 MG1655; (iii) Cm resistance gene amplified from pDG1662[2] with oligos JLG-187 and JLG-188.

pJLG101. This plasmid was constructed by assembling the following 4 fragments by Gibson Assembly (New England Biolabs): (i) the last 881 bp of the *accA* coding sequence (not including the stop codon) amplified with primers JLG-350 and JLG-351 from genomic DNA of *B. subtilis* PY79; (ii) *ssrA***Ωkan* fragment amplified with primers JLG-7 and JLG-184 from pJLG3[3]; (iii) a fragment of 894 bp corresponding to the region immediately downstream of the *accA* stop codon, amplified with primers JLG-352 and JLG-353 from genomic DNA of *B. subtilis* PY79; and (iv) a DNA fragment encompassing the spectinomycin resistant gene, the origin of replication, and the ampicillin resistant gene from pDG1662[2], amplified with primers JLG-95 and JLG-96.

pJLG103. This plasmid was constructed by assembling the following 4 fragments by Gibson Assembly (New England Biolabs): (i) the 810 bp immediately upstream of the *fabZ* stop codon (not including the stop codon) amplified with primers JLG-362 and JLG-363 from genomic DNA of *B. subtilis* PY79; (ii) *ssrA***Ωkan* fragment amplified with primers JLG-7 and JLG-184 from pJLG3[3]; (iii) a fragment of 838 bp corresponding to the region immediately downstream of *fabZ* stop codon, amplified with primers JLG-364 and JLG-365 from genomic DNA of *B. subtilis* PY79; and (iv) a DNA fragment encompassing the spectinomycin resistant gene, the origin of replication, and the ampicillin resistant gene from pDG1662[2], amplified with primers JLG-95 and JLG-96.

pJLG110. This plasmid was constructed by assembling the following 4 fragments by Gibson Assembly (New England Biolabs): (i) the last 782 bp of the *dnaN* coding sequence (not including the stop codon) amplified with primers JLG-404 and JLG-405 from genomic DNA of *B. subtilis* PY79; (ii) *ssrA***Ωkan* fragment amplified with primers JLG-7 and JLG-184 from pJLG3[3]; (iii) a fragment of 813 bp corresponding to the region immediately downstream of the last amino acid-coding codon of *dnaN*, amplified with primers JLG-406 and JLG-407 from genomic DNA of *B. subtilis* PY79; and (iv) a DNA fragment encompassing the spectinomycin resistant gene, the origin of replication, and the ampicillin resistant gene from pDG1662[2], amplified with primers JLG-95 and JLG-96.

pJLG184. This plasmid was constructed by assembling the following 4 fragments by Gibson Assembly (New England Biolabs): (i) the last 682 bp of the *racE* coding sequence (not including the stop codon) amplified with primers JLG-763 and JLG-764

from genomic DNA of *B. subtilis* PY79; (ii) *ssrA**Ω*kan* fragment amplified with primers JLG-7 and JLG-184 from pJLG3[3]; (iii) a fragment of 736 bp corresponding to the region immediately downstream of the last amino acid-coding codon of *racE*, amplified with primers JLG-765 and JLG-766 from genomic DNA of *B. subtilis* PY79; and (iv) a DNA fragment encompassing the spectinomycin resistant gene, the origin of replication, and the ampicillin resistant gene from pDG1662[2], amplified with primers JLG-95 and JLG-96.

pJLG331. This plasmid was constructed by assembling the following 4 fragments by Gibson Assembly (New England Biolabs): (i) the last 831 bp of the *murAA* coding sequence (not including the stop codon) amplified with primers JLG-428 and JLG-429 from genomic DNA of *B. subtilis* PY79; (ii) *ssrA**Ω*kan* fragment amplified with primers JLG-7 and JLG-184 from pJLG3[3]; (iii) a fragment of 910 bp corresponding to the region immediately downstream of the *murAA* stop codon, amplified with primers JLG-430 and JLG-431 from genomic DNA of *B. subtilis* PY79; and (iv) a DNA fragment encompassing the spectinomycin resistant gene, the origin of replication, and the ampicillin resistant gene from pDG1662[2], amplified with primers JLG-95 and JLG-96.

pER114. This plasmid was constructed by assembling the following 4 fragments by Gibson Assembly (New England Biolabs): (i) the last 664 bp of *ytsJ* coding sequence (not including the stop codon) amplified with primers oER369 and oER372 from genomic DNA of *B. subtilis* PY79; (ii) *sfGFP-ssrA**Ω*kan* fragment amplified with primers JLG-7 and JLG-77 from pJLG36 [3]; (iii) a fragment of 595 bp corresponding to the region immediately downstream of the *ytsJ* stop codon, amplified with primers oER373 and oER374 from genomic DNA of *B. subtilis* PY79; and (iv) a DNA fragment encompassing

the spectinomycin resistant gene, the origin of replication, and the ampicillin resistant gene from pDG1662[2], amplified with primers JLG-95 and JLG-96.

Minimal inhibitory concentration determination. Minimal inhibitory concentration (MIC), listed in Table S2, was determined by the microdilution method. Cultures were grown as for microscopy, except they were allowed to reach a final OD600 of 0.2 and then diluted 1:100 into a 96 well plate with different antibiotic concentrations. MICs were determined at 30℃.

YtsJ-GFP-ssrA* degradation measurement. To monitor the degradation of YtsJ-GFP-ssrA*, fluorescence microscopy was performed as described above, except SYTOX Green was not used and microscopy was performed every 15 minutes for 1 hour. After microscopy, the FM 4-64 images were used to identify cells via CellProfiler v. 2.1.1[4] and intensity of the YtsJ-GFP-ssrA* in the identified cells was measured on undeconvolved images. Cells without YtsJ-GFP-ssrA* (PY79) were used as a background control. The mean fluorescence intensity of each cell was averaged and the intensity of the cells without YtsJ-GFP-ssrA* subtracted. Any numbers that fell below 0 were set to 0. This value was then divided by the mean YtsJ-GFP-ssrA* intensity at the 0 minute timepoint to get percent fluorescence.

Generation of cell morphology measurements. All z-stack images were processed into tifs and medial focal planes determined. Tifs were created in Fiji and adjusted in Photoshop (CS6) to facilitate later identification of objects during thresholding. Images were then analyzed using CellProfiler v. 2.1.1[4]. Cells were initially identified using the FM 4-64 images and the objects were expanded using the phase image as a guide to obtain final cell objects. Nucleoids were identified separately and then associated with

corresponding cells. Two different cell types were defined: cells containing nucleoids and anucleate cells. Cell parameters were measured using cells containing nucleoids for most treatments, however, some treatments result in anucleate cells (i.e. ciprofloxacin) or difficult to detect nucleoids (i.e. D-cycloserine) and in those cases, anucleate cells were included in cell measurements (indicated in Table S6). Size and shape properties were measured for all objects, as well as DAPI and SYTOX Green intensities (measured on unadjusted undeconvolved images). The measured parameters used for analysis and their definitions are listed in Table S5. All measurements are for cells grown in LB, measurements were not made for cells grown in LBMSM. All parameters used for analysis are population averages of ≥100 objects (with a few exceptions listed in supporting information). Cell parameters used in the bar graphs in Figure 3 were counted manually in Fiji. Lysed cells were defined as cells with visible gaps in FM 4-64 staining and above background SYTOX green intensity (≥140 without background correction). Retracted septa were defined as septa where the edge of the cell as defined by phase contrast was visibly bigger than that defined by the FM4-64 staining, as is shown in Figure 3J (AZ105, cerulenin, AccA-ssrA*). All graphs show the average of ≥3 separate experiments and error bars represent the standard deviation between experiments.

Line intensity analysis. The intensity of FM 4-64 staining along the membrane was measured on undeconvolved images in Fiji[5]. A line was drawn across a membrane segment (avoiding the septum) and the intensity measured and output as a text file. The background intensity (measured on an area with no cells) was subtracted from each value, and each value was divided by the average of the intensity over the entire

segment. Lastly, the ratio was adjusted by subtraction so the highest ratio in each segment was equal to 1.

Blinded Test. Antibiotics (excluding the membrane active category) and degradation strains from all pathways tested were included in a blinded experiment. Antibiotics and degradation strains were blinded separately. Cell measurements from all blinded antibiotic treatments after 2 hours of treatment were scored using the combined LDA coefficient matrix and these scores were added to the scatterplots and clustered based on Euclidean distance. Microscopy was performed on degradation strains every hour for 3 hours. The data was then analyzed and scored using the combined LDA coefficient matrix and the scores were clustered based on Euclidean distance. The earliest timepoint for each blinded strain that clustered most closely with a defined pathway was chosen (Figure S2) and then graphed on the scatterplot. For AccA, the 2 hour timepoint was used instead of the 1 hour timepoint due to the appearance of FM 4-64 staining gaps at 2 hours.

Viable cell counts. Viable cell counts were obtained through dilution and plating of cells from the same cultures as those subjected to microscopy. Ten-fold serial dilutions were made in 1X Tbase at initial treatment (t_0) and after 4 hours of treatment (t_4) and spotted onto LB plates. Colonies were counted after growth and colony forming units (cfu) per ml calculated. The ratio of cfus per ml of each treatment at 4 hours (cfu t_4) to the solvent control at 0 hours ($cfu^C\ t_0$) was calculated and then converted to log base 10 units.

Linear discriminant and clustering analysis. Linear discriminant analysis (LDA) was completed using a built-in MATLAB (v.R2014b) function. Before graphing, the scores

for the top three LDA parameters were shifted so each parameter centered at 0. The same shift was applied to all subsequent scoring using the same coefficient matrix. The scores of the top three (top two for the nucleoid matrix) LDA parameters generated from the LDA coefficient matrix were used for Euclidean distance hierarchical clustering (average linkage) in MultiExperiment Viewer v4.9.0. For antibiotic categories other than membrane active, measurements after 2 hours of treatment were used. For degradation strains, the timepoint with the best phenotype was selected. For data included in the nucleoid matrix, measurements of cells treated for 10 minutes were used.

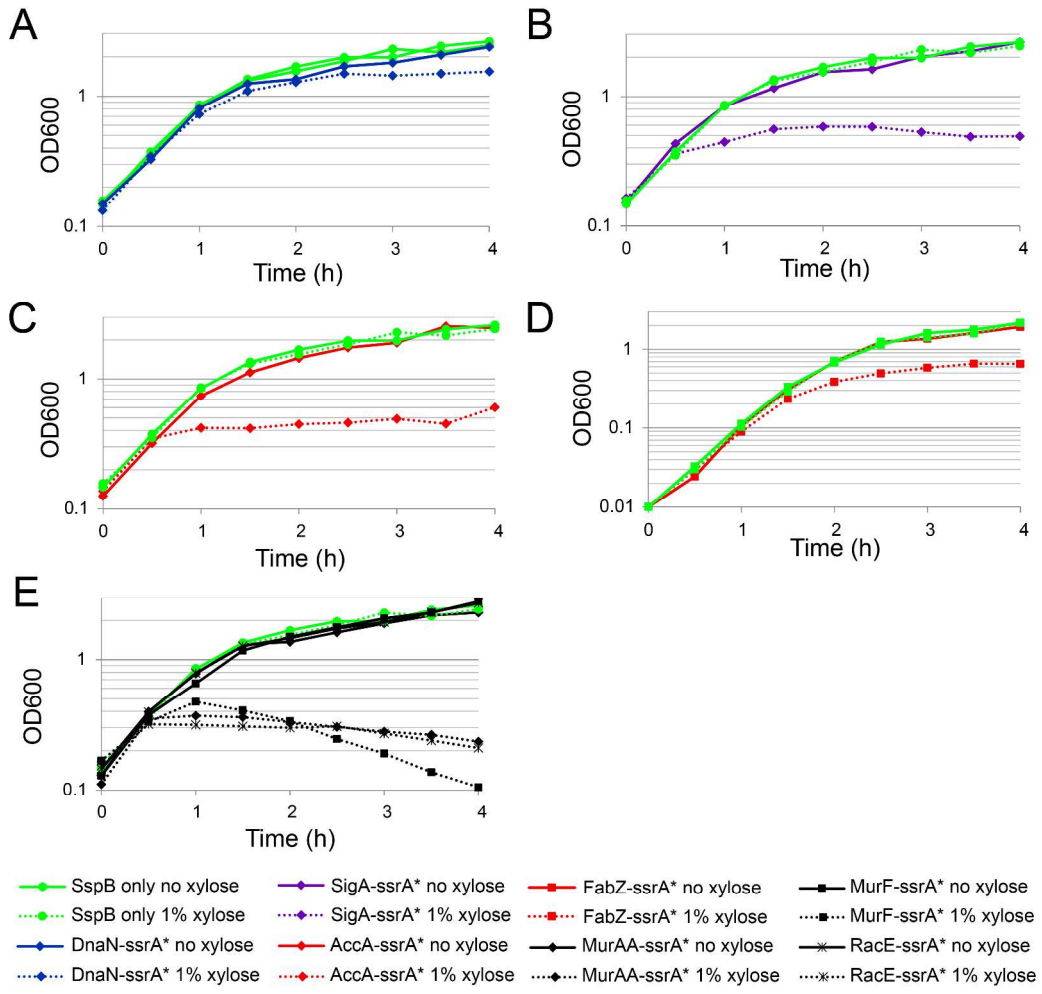

Figure S1. Effect of degradation of essential proteins on growth rate. (A-D) Representative growth curves of strains containing ssrA*-tagged protein (A) DnaN (B) SigA (C) AccA (D) FabZ (E) MurAA, MurF, RacE. Dotted lines indicate addition of xylose. All graphs also contain an SspB* only control (green).

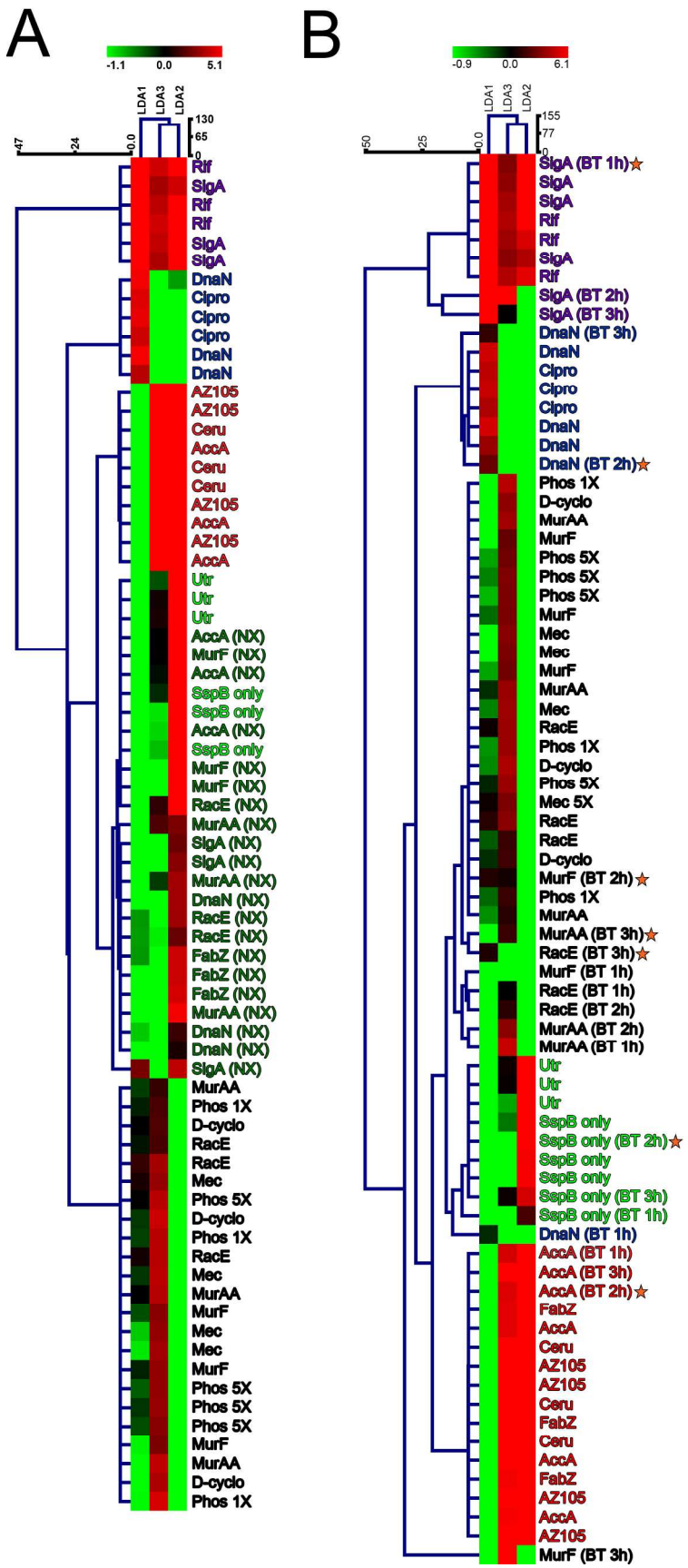

Figure S2. Euclidean distance hierarchical clustering of LDA score. (A) Euclidean distance hierarchical clustering of LDA1, LDA2 and LDA3 scores of antibiotic treated cells (2 h) and degradation strains (selected timepoints) with and without addition of xylose using the combined LDA matrix. NX signifies no xylose was added, and thus no degradation occurred. (B) Euclidean clustering of LDA1, LDA2 and LDA3 scores of antibiotic treated cells (2 h), degradation strains (selected timepoints) and all timepoints of the blinded control ssrA*-tagged strains using the combined LDA matrix. Treatment names are color-coded based on pathway affected: Controls (green), Replication (blue), Transcription (purple), Fatty acid biosynthesis (red), Peptidoglycan (black). BT indicates blinded test data. Orange stars indicated timepoint picked for each blinded test that is used for LDA in Figure 6. Data used to generate trees can be found in Tables S6 and S8. Antibiotic concentrations and abbreviation key can be found in Table S2.

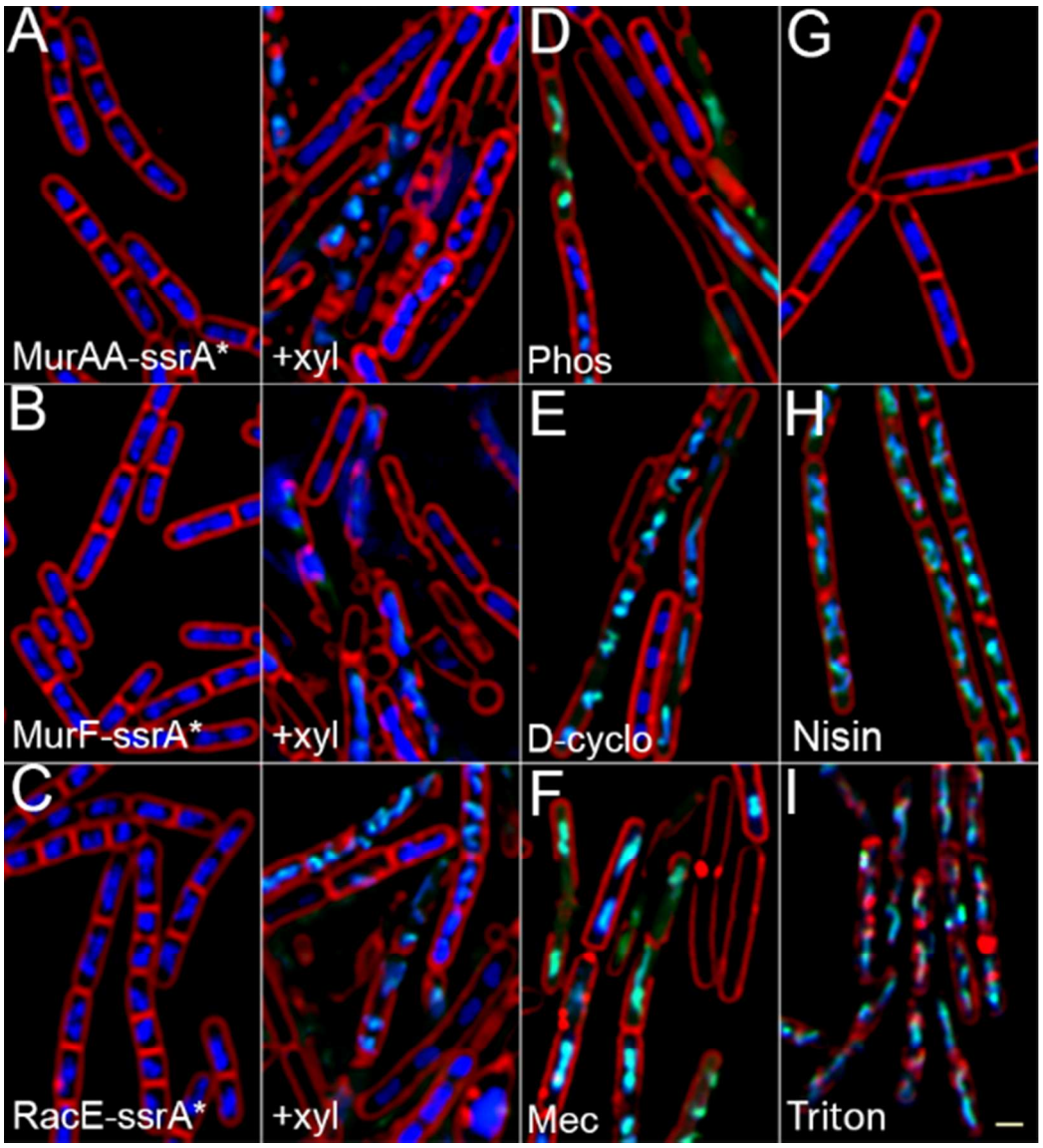

Figure S3. RIP of proteins involved in peptidoglycan biosynthesis, and comparison to control antibiotics. (A) Cells containing ssrA*-tagged MurAA without and with degradation after 3 h. (B) Cells containing ssrA*-tagged MurF without and with degradation after 2 h. (C) Cells containing ssrA*-tagged RacE without and with degradation after 3 h. (D-I) PY79 cells treated with antibiotics. Cells were treated for either 2 h (D-F) or 30 min (G-I) with phosphomycin (D), D-cycloserine (E), mecillinam (F), nisin (H), triton (I) at 1X MIC (E,H) or 5X MIC (D,F,I) or left untreated (G). Cells are stained with FM 4-64 (red), DAPI (blue), and SYTOX Green (green). Scale bar represents 1 µm. MIC values are contained in Table S2.

REFERENCES

1. Becker, E., Herrera, N. C., Gunderson, F. Q., Derman, A. I., Dance, A. L., Sims, J., Larsen, R. A., and Pogliano, J. (2006) DNA segregation by the bacterial actin AlfA during Bacillus subtilis growth and development, *EMBO J 25*, 5919-5931.
2. Guerout-Fleury, A. M., Frandsen, N., and Stragier, P. (1996) Plasmids for ectopic integration in Bacillus subtilis, *Gene 180*, 57-61.
3. Yen Shin, J., Lopez-Garrido, J., Lee, S. H., Diaz-Celis, C., Fleming, T., Bustamante, C., and Pogliano, K. (2015) Visualization and functional dissection of coaxial paired SpoIIIE channels across the sporulation septum, *Elife 4*, e06474.
4. Carpenter, A. E., Jones, T. R., Lamprecht, M. R., Clarke, C., Kang, I. H., Friman, O., Guertin, D. A., Chang, J. H., Lindquist, R. A., Moffat, J., Golland, P., and Sabatini, D. M. (2006) CellProfiler: image analysis software for identifying and quantifying cell phenotypes, *Genome Biol 7*, R100.
5. Schindelin, J., Arganda-Carreras, I., Frise, E., Kaynig, V., Longair, M., Pietzsch, T., Preibisch, S., Rueden, C., Saalfeld, S., Schmid, B., Tinevez, J. Y., White, D. J., Hartenstein, V., Eliceiri, K., Tomancak, P., and Cardona, A. (2012) Fiji: an open-source platform for biological-image analysis, *Nat Methods 9*, 676-682.